Angewandte Chemie
Eine Zeitschrift der Gesellschaft Deutscher Chemiker

Supporting Information

A Highly Stable and Non-Flammable Deep Eutectic Electrolyte for High-Performance Lithium Metal Batteries

L. Zhao, A. Xu, Y. Cheng, H. Xu, L. Xu, L. Mai**

Supporting Information

A Highly Stable and Non-Flammable Deep Eutectic Electrolyte for High-Performance Lithium Metal Batteries

Li Zhao [a], *Ao Xu* [a], *Yu Cheng* [a], *Hantao Xu* [a], *Lin Xu* [a, b, c, *], *and Liqiang Mai* [a, b, c, *]

Keywords: dimethylmalononitrile, nitrile group, deep eutectic electrolytes, stable interfacial compatibility, lithium metal batteries

1. Experimental section

1.1. Materials and chemicals

All reagents were purchased and used without further purification. Poly (vinylidene fluoride-co-hexafluoropropylene) (PVDF-HFP, M_w ~455,000, Aladdin), polyethylene oxide (PEO, Mv ~600,000, Sigma-Aldrich), dimethylmalononitrile (DMMN, 98%, Aladdin), fluoroethylene carbonate (FEC，99%, Aladdin), lithium bis(trifluoromethan esulfonyl)amide (LiTFSI, 99%, Dodochem), anhydrous ethanol (99.5%, Sinopharm Chemical Reagent), N, N-dimethylformamide (DMF, 99%, Sinopharm Chemical Reagent), liquid electrolyte (1 M $LiPF_6$ was dissolved in ethylene carbonate/ethylmethyl carbonate/dimethyl carbonate (EC/EMC/DMC, 1/1/1 by weight), Dodochem).

1.2. Preparation of deep eutectic electrolytes (DEEs)

First, a variety of eutectic compositions were synthesized by heating LiTFSI (T_m = 238 ℃) and DMMN (T_m = 32 ℃) at 60 ℃, forming a uniform and transparent light-yellow solution. Subsequently, the additive FEC, which constitutes 5% of the weight of LiTFSI, was incorporated. The solution was cooled to obtain DEEs with varying molar ratios. These DEEs were stored in an argon-filled glove box with oxygen and water contents lower than 0.1 ppm.

1.3. Preparation of PHPDEE polymer electrolytes

The PVDF-HFP (1000 mg), PEO (100 mg), and LiTFSI (1000 mg) were combined with 9.0 mL of DMF in a 20 mL capacity vial, followed by the addition of 1.0 mL of anhydrous ethanol. The vial was sealed and placed on a heating stage, where it was vigorously stirred at 60 ℃ for

24 h to achieve a homogeneous solution. Subsequently, the solution was cast onto a glass slide at room temperature. The resulting electrolytes were then dried in an oven at 80 ℃ for 2 h, baked in a vacuum oven at 60 ℃ for 24 h to remove the solvent to obtain the PVDF-HFP, PEO composite polymer electrolyte (PHPCPE), and stored in a glovebox for further analysis.

As a carrier of DEE, PHPCPE has the advantages of high strength and good wettability, which can effectively prevent battery short circuits and improve battery cycle stability. In addition, LiTFSI in PHPCPE reacts easily with DMMN in DEE, which improves the infiltration effect of DEE in PHPCPE.

The PHPDEE polymer electrolyte was prepared by the simple coating method in the glove box. After adding 106 mg of DEE-1:6 electrolyte to the surface of PHPCPE with a diameter of 17 mm, the PHPCPE was impregnated with DEE-1:6 electrolyte and brought into contact with its LiTFSI. The reaction between DMMN in the DEE-1:6 electrolyte and LiTFSI was accelerated by heating at 60℃ for 0.5 h, resulting in the formation of PHPDEE-1:4 polymer electrolyte.

1.4. Preparation of $LiFePO_4$ (LFP) cathode and the LFP‖Li battery assembly

Commercial LFP, super-P, and PVDF were mixed in N-methyl pyrrolidone (NMP) with a mass ratio of 7:2:1 to form a uniform slurry, which was subsequently coated on carbon-coated Al foil. The prepared electrode films were dried at 80 ℃ for 24 h under vacuum before battery fabrication, and the active material loading of the LFP cathode is 1.1-1.7 mg cm^{-2}. Finally, different PHPDEEs were sandwiched between LFP cathode and Li metal anode to assemble

the LFP‖Li batteries. Electrochemical tests of LFP‖Li batteries were tested at room temperature in the voltage range of 2.5–4.0 V.

1.5. Preparation of $LiNi_{0.8}Co_{0.1}Mn_{0.1}O_2$ (NCM811) cathode and the NCM811‖Li battery assembly

Commercial NCM811, super-P, and PVDF were mixed in N-methyl pyrrolidone (NMP) with a mass ratio of 8:1:1 to form a uniform slurry, which was subsequently coated on carbon-coated Al foil. The prepared electrode films were dried at 80 °C for 24 h under vacuum before battery fabrication, and the active material loading of the NCM811 cathode is 1.2-7.0 mg cm^{-2}. Finally, PHPDEEs were sandwiched between NCM811 cathode and Li metal anode to assemble the NCM811‖Li batteries. Electrochemical tests of the NCM811‖Li batteries were tested at room temperature in the voltage range of 2.5–4.2 V and 2.5–4.5 V.

All CR2016 coin cells were assembled in the glove box under an Ar atmosphere with O_2 and H_2O content below 0.1 ppm.

1.6. Materials characterization

The Fourier transform infrared (FTIR) measurements were obtained using Nicolet 6700 (Thermo Fisher Scientific Co., USA). FTIR spectrometer with a wavenumber range from 400 to 4000 cm^{-1}. Raman spectra were obtained using a Renishaw Invia Raman spectrometer with a 633 nm excitation laser. Differential scanning calorimetry (DSC) measurements were performed by the TA-DSC2500 instrument with a heating rate of 10 ℃ min^{-1} from -80 ℃ to 120 ℃. Thermogravimetric analysis (TGA) was performed in the air atmosphere from 30 to 600 ℃ with a heating rate of 10 ℃ min^{-1} using NETZSCH STA 449F5 simultaneous analyzer.

The components of lithium metal surface were identified by X-ray photoelectron spectroscopy (XPS) using an ESCALAB 250Xi instrument. The DEEs were measured by NMR spectroscopy (Bruker 400 MHz, DMSO−d_6) to investigate the electrolyte decomposition reactions. TOF-SIMS measurements were conducted with a PHI nano TOF III. A Bi_3^{++} beam (3 kV, 2 nA) with a raster size of 100 μm was used as the primary beam to detect the samples, sputtering with an Ar^+ beam (2 kV, 100 nA, 400×400 μm^2) was applied for depth profiling analysis.

1.7. Electrochemical measurements

The ionic conductivity was determined by EIS after placing PHPDEE between two electrodes (stainless steel) contacts in a CR2016 coin cell. Autolab PGSTAT302N was used to test EIS with measurements frequency ranges from 10^6 to 1.0 Hz at room temperatures. The ionic conductivity (σ) was calculated using the following equation S1:[1]

$$\boldsymbol{\sigma = \frac{L}{RS}} \qquad \textbf{Equation S1}$$

Where L is the thickness of the polymer electrolyte membranes, R is the bulk resistance of the polymer electrolyte membranes, and S is the area of the stainless steel.

The activation energy for Li^+ transport through SEI was based on the temperature-dependent EIS measurement of Li‖Li cell (20~80°C). The activation energy can be obtained according to the slope of the linear fit of the Arrhenius plot. The Arrhenius equation is shown as equation S2:

$$\boldsymbol{\sigma = A\exp\left(\frac{E_a}{kT}\right)} \qquad \textbf{Equation S2}$$

where σ is the ionic conductivity, A is the pre-reference factor, k is the Boltzmann constant, and T is the absolute temperature.

The electrochemical stability window of the LMB was analyzed through linear sweep voltammetry (LSV) on a Li‖PHPDEE‖stainless steel cell. The voltage scan ranged from the open-circuit voltage to 6.0 V with a scan rate of 10 mV s^{-1}.

The Li-ion transference number (t_{Li^+}) was tested in a symmetric lithium cell using an Autolab PGSTAT302N at room temperature by a combination of DC polarization and AC impedance measurement. A DC potential (ΔV=10 mV) was applied for 5500 s to gain the initial and steady currents. Meanwhile, the AC impedance spectra of the same cell were measured before and after polarization. The value of lithium transference number (t_{Li^+}) has been calculated by the following equation S3: [1a, 2]

$$\boldsymbol{t_{Li^+} = \frac{I_{ss}(\Delta V - I_0 R_0)}{I_0(\Delta V - I_{ss} R_{ss})}} \qquad \textbf{Equation S3}$$

Where the ΔV is the polarization voltage, I_0 and R_0 are the current and resistance of the initial state, and the I_{ss} and R_{ss} are the current and resistance of the stable state, respectively.

The cycling stability of PHPDEEs against lithium metals was measured by a Li‖Li symmetric cell using a LAND CT2001A charge/discharge system at room temperature. The cycling stability and specific capacity of full batteries with PHPDEEs were conducted using a multichannel battery testing system (LAND CT2001A).

2. Supplementary figures

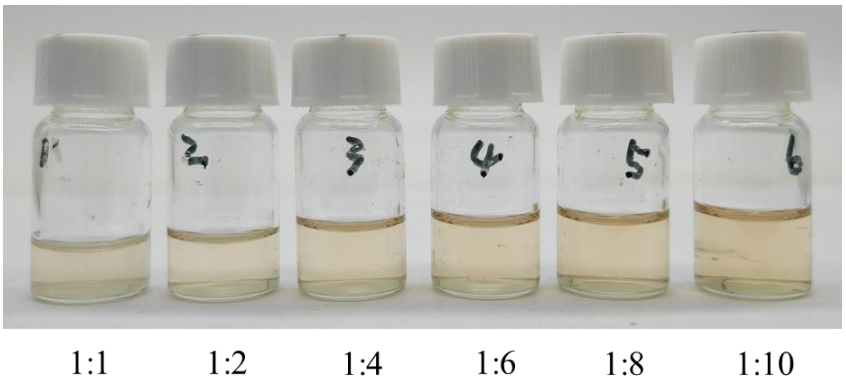

Figure S1. Photos of DEEs at various molar ratios.

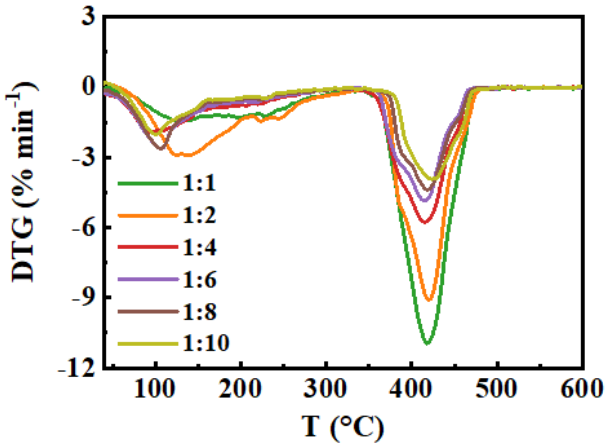

Figure S2. Derivative thermogravimetric (DTG) spectra of DEEs from 30 ℃ to 600 ℃ with a heating rate of 10 ℃ min^{-1} under a nitrogen atmosphere.

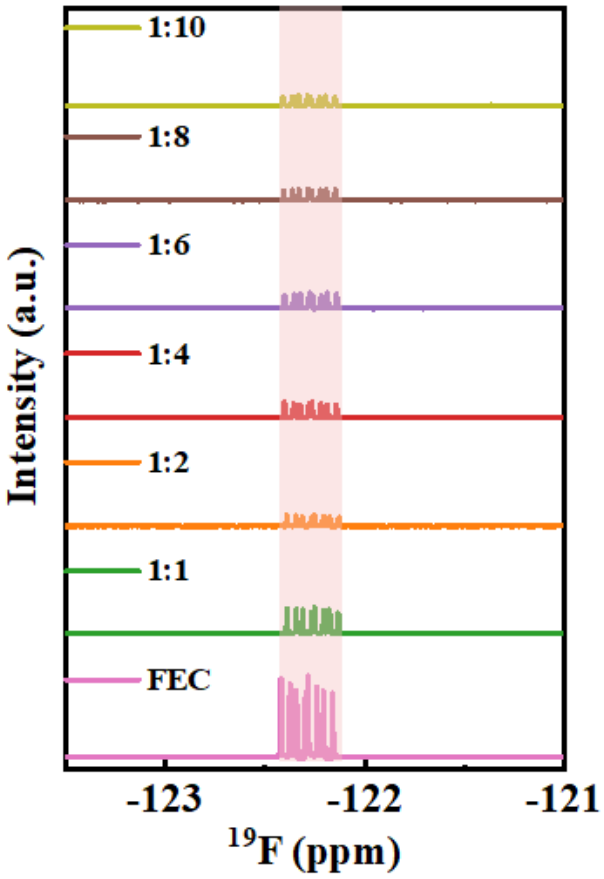

Figure S3. NMR spectra of FEC and varying molar ratios of DEEs.

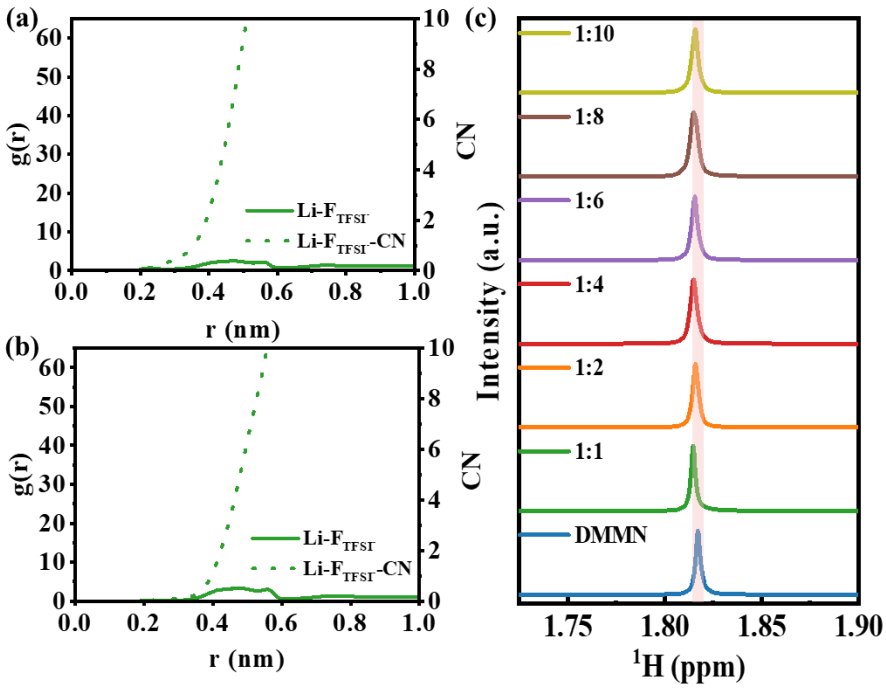

Figure S4. a)-b) The radial distribution function of DEE-1:1 and DEE-1:4. c) NMR spectra of LiTFSI, LiTFSI in DMMN.

Table S1. Radial distribution function (r) and coordination number (CN) between Li^+, anions, and solvent molecules in the DEE-1:1 and DEE-1:4 systems.

Scheme	$Li\text{-}F_{TFSI}$- (DEE-1:1)	$Li\text{-}F_{TFSI}$- (DEE-1:4)
r	2.22 Å	2.28 Å
CN	0.442	0.096

Table S2. Radial distribution function (r) and coordination number (CN) between Li^+, anions, and solvent molecules in the DEE-1:1 and DEE-1:4 systems.

Scheme		Li-O_{TFSI}-	Li-N_{DMMN}
DEE-1:1	r	2.02 Å	2.26 Å
	CN	3.669	0.969
DEE-1:4	r	2.02 Å	2.60 Å
	CN	3.268	1.781

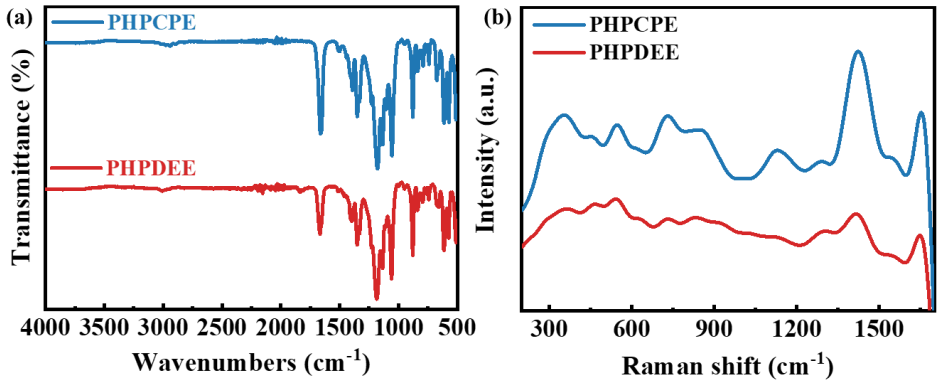

Figure S5. a)-b) FTIR and Raman spectra of PHPCEE and PHPDEE.

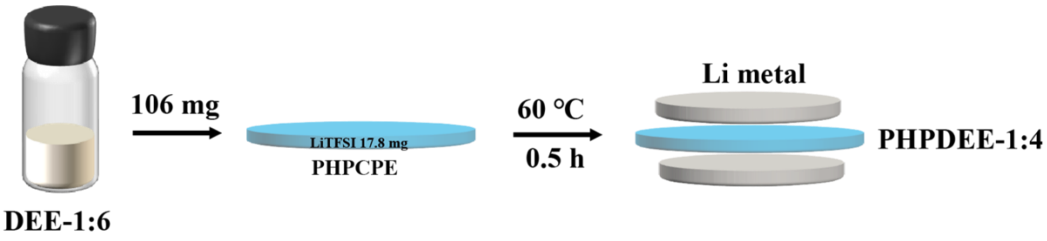

Figure S6. Diagram of the preparation process of the polymer electrolytes (PHPDEE-1:4).

A certain amount of DEE-1:6 electrolyte was added to the surface of PHPCPE. DEE-1:6 infiltrated PHPCPE and encountered its LiTFSI. It was heated at 60 ℃ for 0.5 h to accelerate the reaction between DMMN in DEE-1:6 and LiTFSI, thereby obtaining PHPDEE-1:4 polymer electrolyte.

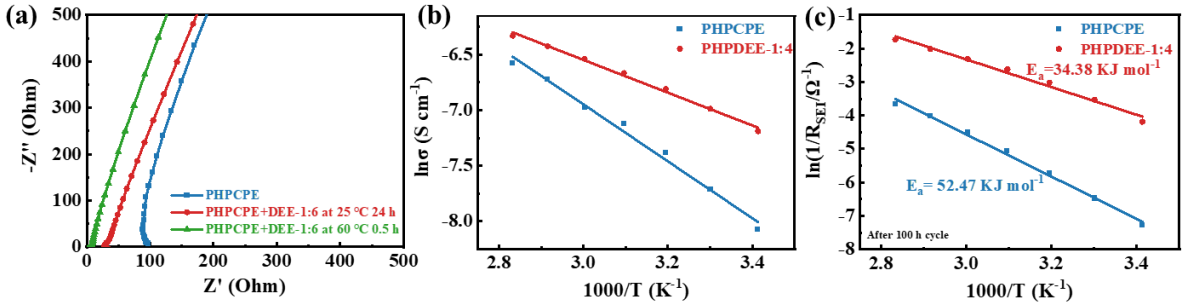

Figure S7. a) Nyquist plots of the polymer electrolytes collected from PHPDEE-1:6 to PHPDEE-1:4 at 60°C. b) Temperature-dependent ionic conductivity of the PHPDEE-1:4. c) The activation energies for ion diffusion through SEI were determined by fitting RSEI obtained at room temperature using the Arrhenius equation.

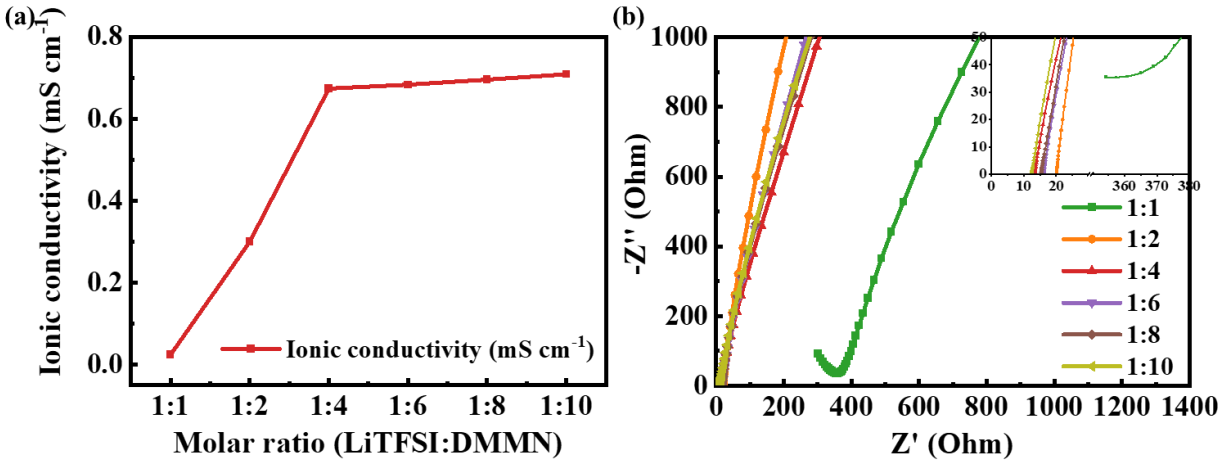

Figure S8. a) Ionic conductivity of the PHPDEEs at different molar ratios. b) Nyquist plots of the PHPDEEs collected at different molar ratios.

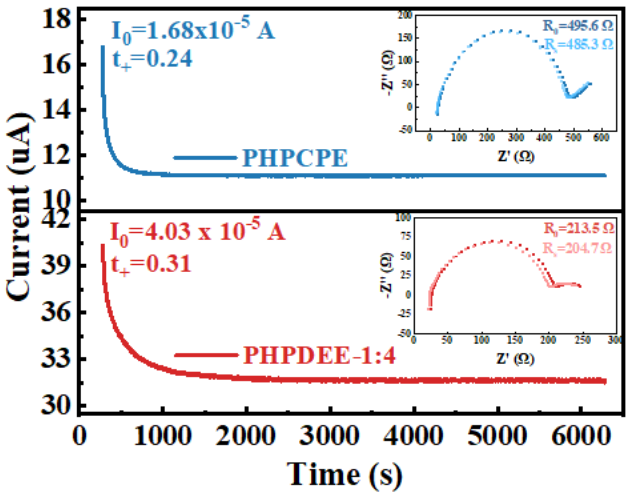

Figure S9. Direct current polarization profile of Li‖Li symmetric cell with PHPDEE-1:4.

Table S3. The transference numbers of lithium ions in PHPDEE-1:4.

Scheme	PHPCPE	PHPDEE-1:4
R_0 [Ω]	495.60	213.50
R_{ss} [Ω]	485.30	204.70
I_0 [A]	1.68×10^{-5}	4.03×10^{-5}
I_{ss} [A]	1.11×10^{-5}	3.15×10^{-5}
ΔV [mV]	10.00	10.00
t_{Li+}	0.24	0.31

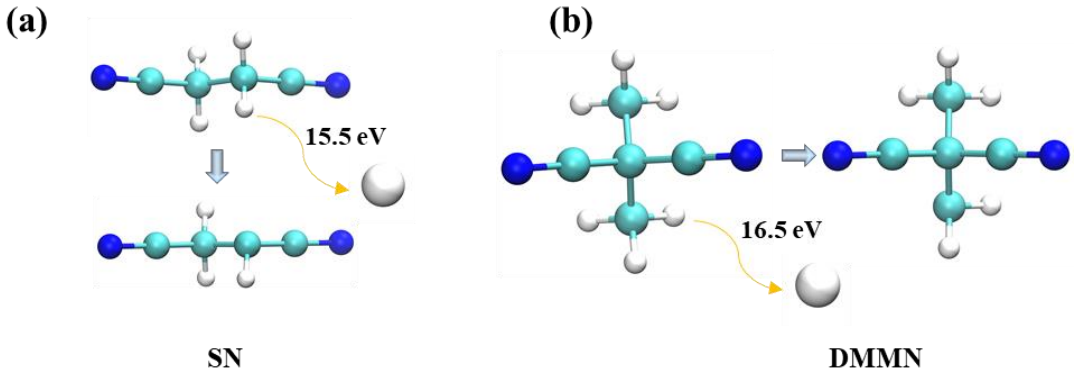

Figure S10. a) C-H bond energy in SN molecule. b) C-H bond energy in DMMN molecule.

Atom colors: H-white, C-cyan, N-blue.

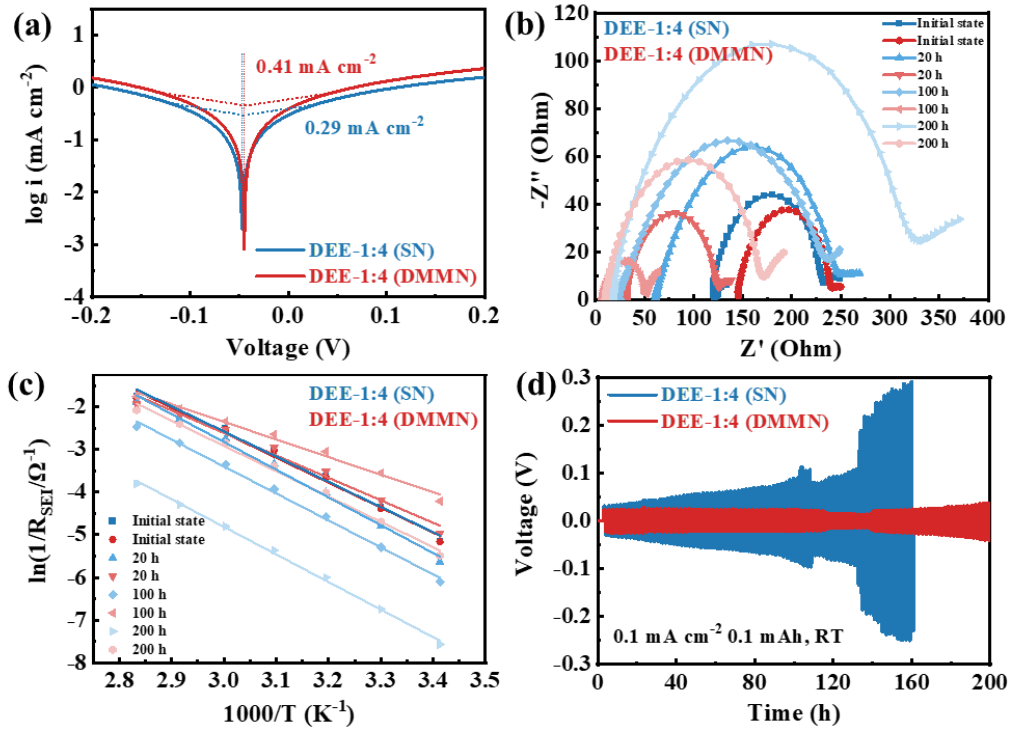

Figure S11. a) Tafel plots obtained from CV test in Li‖Li cells using DEE-1:4 (SN) and DEE-1:4 (DMMN) electrolytes. b) Nyquist plots of the Li‖DEE-1:4‖Li symmetric cells at different cycles. c) The activation energies for ion diffusion through SEI were determined by fitting R_{SEI} obtained in various temperatures (20 to 80 ℃) using the Arrhenius equation. d) Voltage profiles of the Li||Li symmetric cells using the DEE-1:4 at 0.1 mA cm^{-2} for 1 h.

Table S4. Nyquist plots of the Li‖Li symmetric cells at different cycles.

Scheme	R_{EIS}			
	Initial state	20 h	100 h	200 h
DEE-1:4 (SN)	232	250	240	330
DEE-1:4 (DMMN)	240	125	51	170

Table S5. The activation energies in various cycles.

Scheme	Ea (KJ mol^{-1})			
	Initial state	Cycle for 20 h	Cycle for 100 h	Cycle for 200 h
DEE-1:4 (SN)	49.08118	54.13929	52.58401	53.7545
DEE-1:4 (DMMN)	48.65441	43.76159	34.37545	49.35738

Figure S12. Reactivity of lithium metal foil and DEE-1:4 solutions at room temperature.

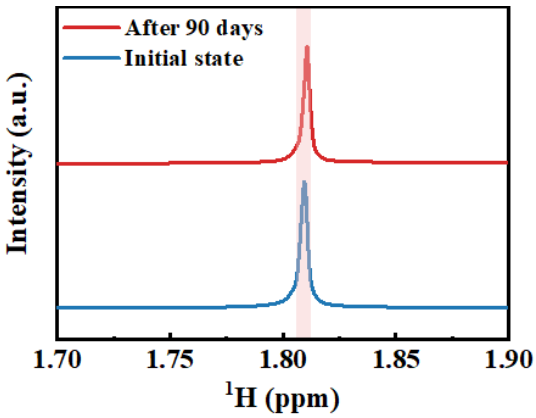

Figure S13. NMR spectra of DEE at various time points.

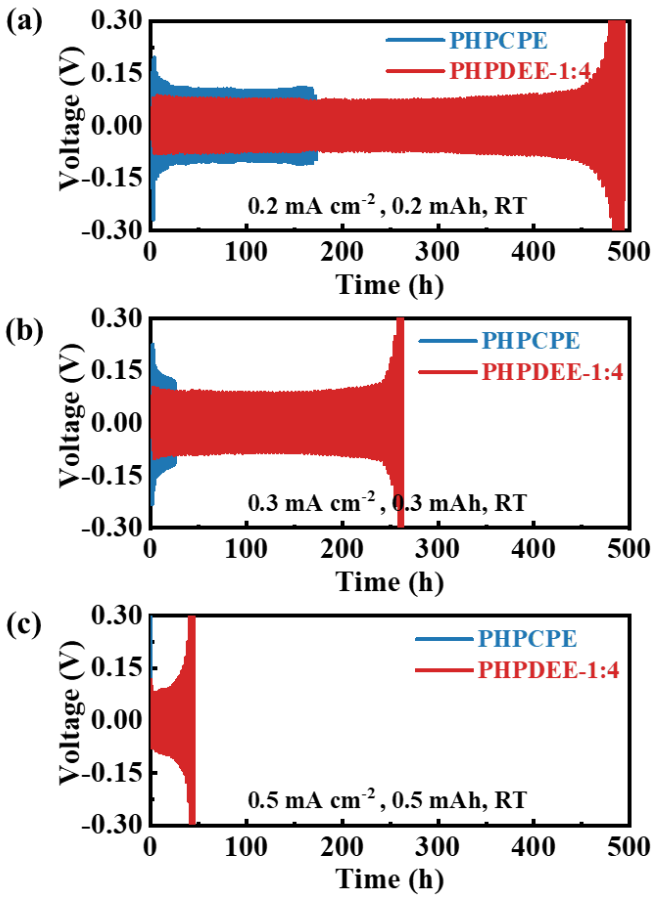

Figure S14. a)-c) Cycling stability of Li||Li symmetric cells with PHPDEE-1:4 from 0.2 to 0.5 mA cm^{-2}.

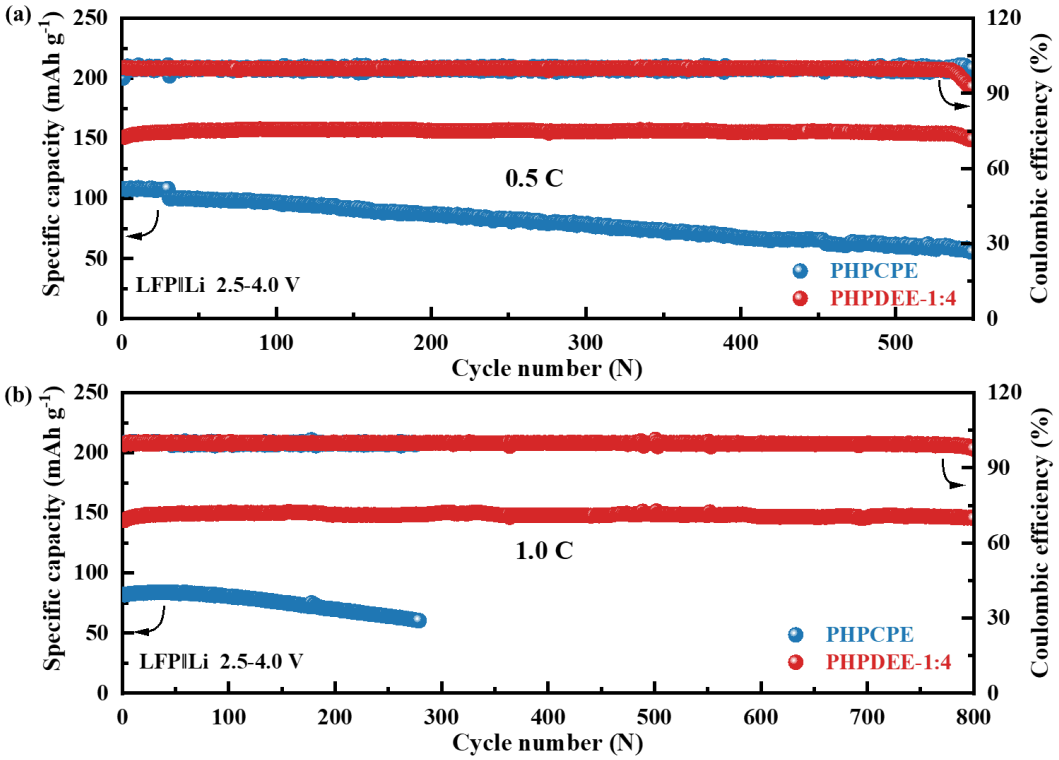

Figure S15. a)-b) Long-term cycling performance of the LFP‖Li batteries at 0.5 C and 1.0 C under room temperature.

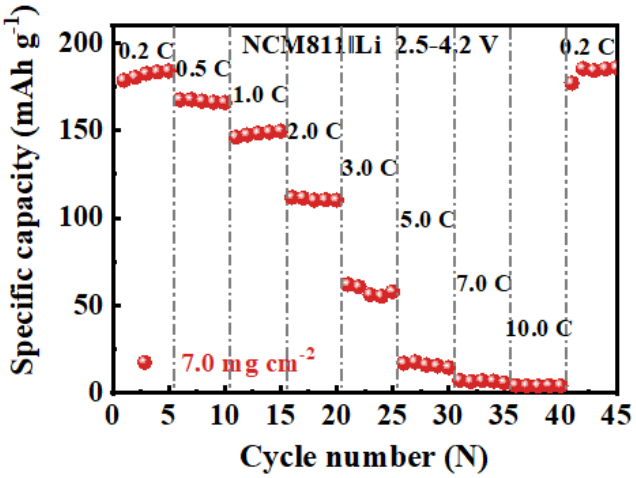

Figure S16. Rate performance profiles of NCM811||Li batteries using DMMN-based DEE with a high-loading NCM811 cathode.

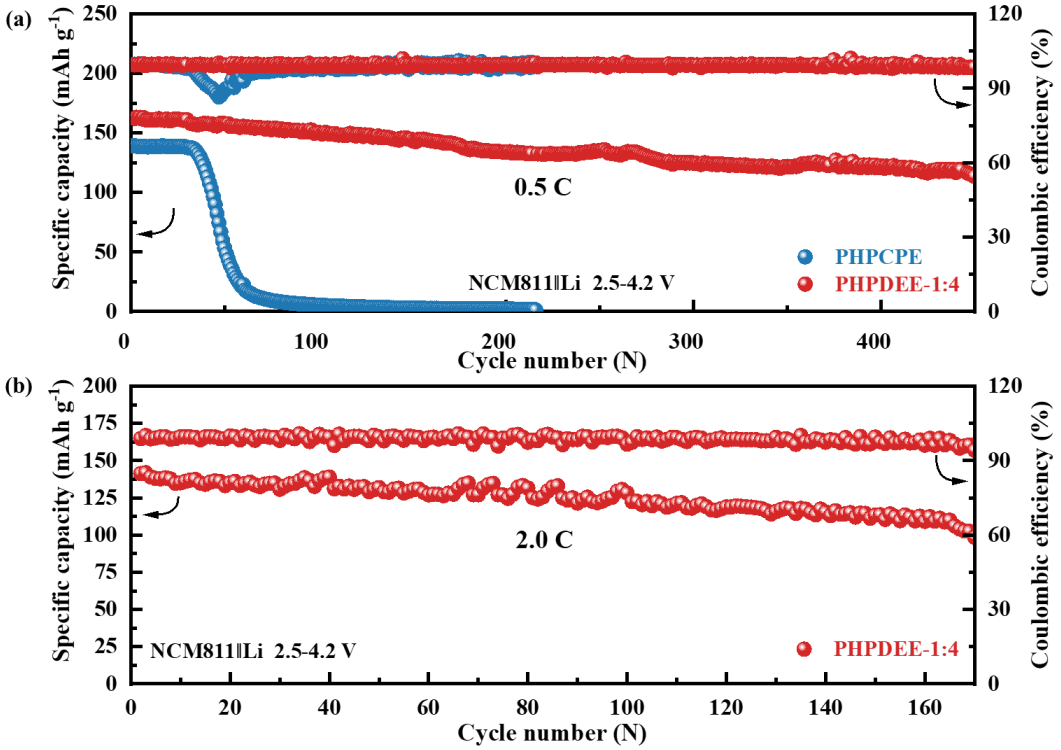

Figure S17. a)-b) Long-term cycling performance of the NCM811‖Li batteries at 0.5 C and 2.0 C under room temperature.

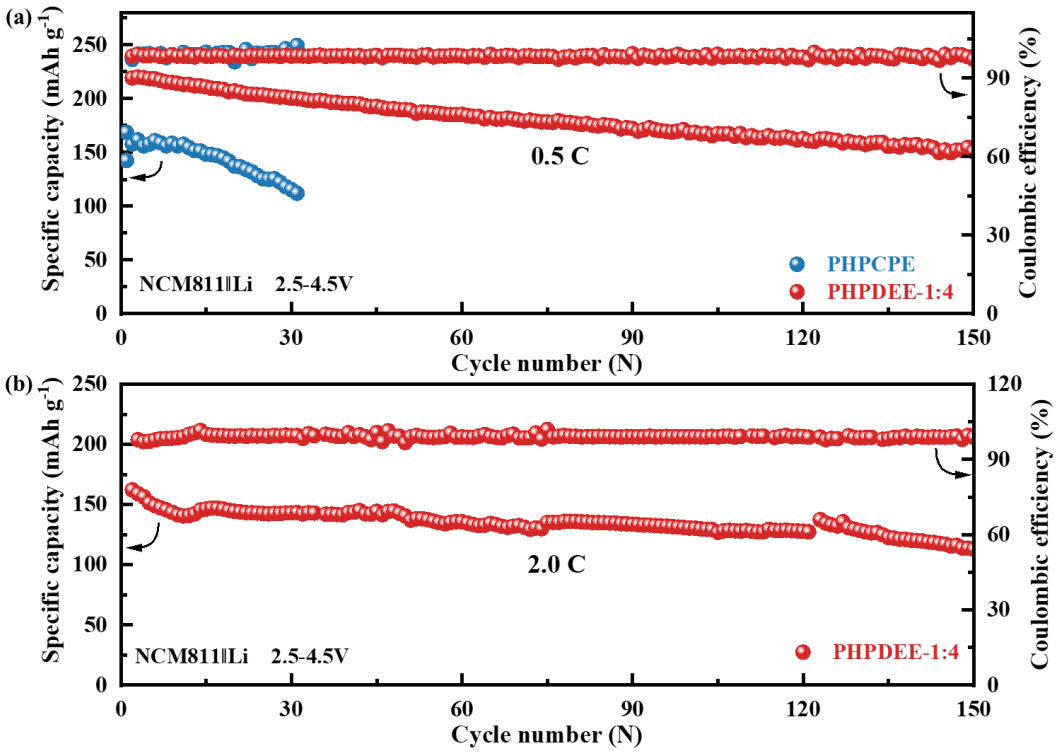

Figure S18. a)-b) Long-term cycling performance of the NCM811‖Li batteries at 0.5 C and 2.0 C under room temperature.

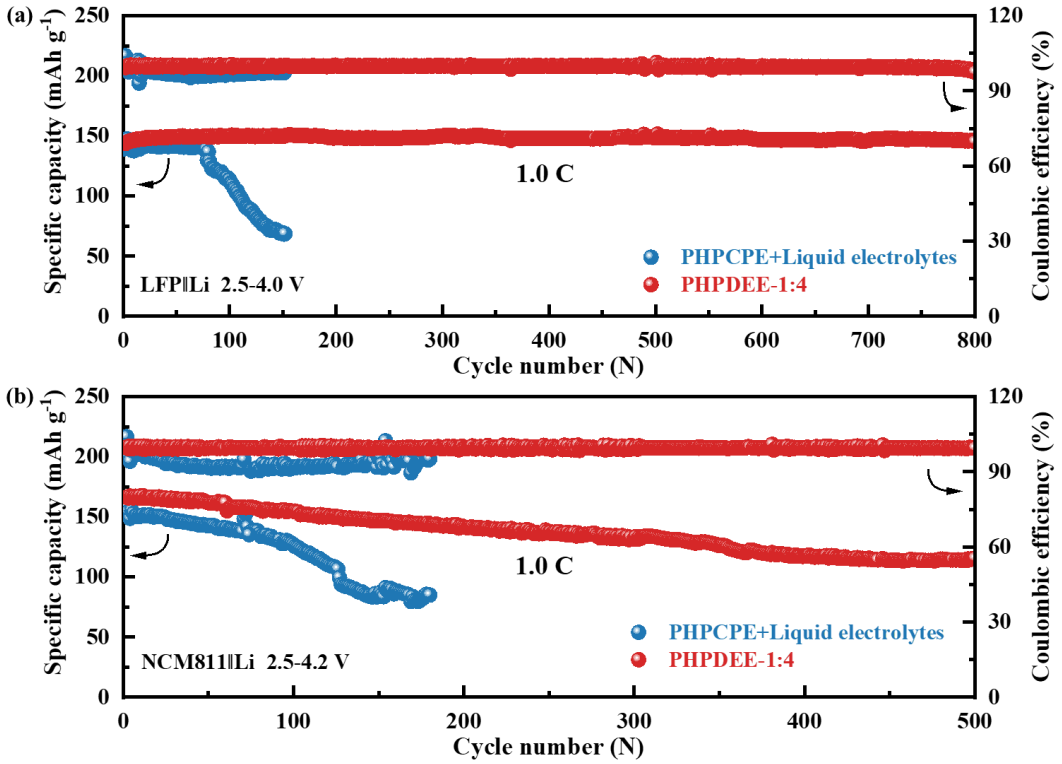

Figure S19. a) Long-term cycling performance of the LFP||Li batteries at 1.0 C under room temperature. b) Long-term cycling performance of the NCM811||Li batteries at 1.0 C under room temperature.

References

[1] a) W. J. Hyun, C. M. Thomas, N. S. Luu, M. C. Hersam, *Adv. Mater.* **2021**, *33*, e2007864;

b) X. Fu, M. J. Hurlock, C. Ding, X. Li, Q. Zhang, W. H. Zhong, *Small* **2022**, *18*, e2106225;

c) W. Chen, R. V. Salvatierra, M. Ren, J. Chen, M. G. Stanford, J. M. Tour, *Adv. Mater.* **2020**, *32*, e2002850.

[2] M. J. Lee, J. Han, K. Lee, Y. J. Lee, B. G. Kim, K. N. Jung, B. J. Kim, S. W. Lee, *Nature* **2022**, *601*, 217-222.